ANTIMICROBIAL AGENTS AND CHEMOTHERAPY, Apr. 2009, p. 1610–1618 Vol. 53, No. 4
0066-4804/09/$08.00+0 doi:10.1128/AAC.01040-08

The Lipopeptide Antibiotic Friulimicin B Inhibits Cell Wall Biosynthesis through Complex Formation with Bactoprenol Phosphate▽

T. Schneider,[1]* K. Gries,[1] M. Josten,[1] I. Wiedemann,[1] S. Pelzer,[2]§ H. Labischinski,[2] and H.-G. Sahl[1]

Institute of Medical Microbiology, Immunology and Parasitology, Pharmaceutical Microbiology Section, University of Bonn, Meckenheimer Allee 168, D-53115 Bonn, Germany,[1] and MerLion Pharmaceuticals GmbH, Robert-Roessle-Str. 10, D-13125 Berlin, Germany[2]

Received 4 August 2008/Returned for modification 6 November 2008/Accepted 10 December 2008

Friulimicin B is a naturally occurring cyclic lipopeptide, produced by the actinomycete *Actinoplanes friuliensis*, with excellent activity against gram-positive pathogens, including multidrug-resistant strains. It consists of a macrocyclic decapeptide core and a lipid tail, interlinked by an exocyclic amino acid. Friulimicin is water soluble and amphiphilic, with an overall negative charge. Amphiphilicity is enhanced in the presence of Ca^{2+}, which is also indispensable for antimicrobial activity. Friulimicin shares these physicochemical properties with daptomycin, which is suggested to kill gram-positive bacteria through the formation of pores in the cytoplasmic membrane. In spite of the fact that friulimicin shares features of structure and potency with daptomycin, we found that friulimicin has a unique mode of action and severely affects the cell envelope of gram-positive bacteria, acting via a defined target. We found friulimicin to interrupt the cell wall precursor cycle through the formation of a Ca^{2+}-dependent complex with the bactoprenol phosphate carrier C_{55}-P, which is not targeted by any other antibiotic in use. Since C_{55}-P also serves as a carrier in teichoic acid biosynthesis and capsule formation, it is likely that friulimicin blocks multiple pathways that are essential for a functional gram-positive cell envelope.

The lipopeptide antibiotic friulimicin B is produced by the actinomycete *Actinoplanes friuliensis.* It belongs to a class of natural compounds which are highly active against a broad range of gram-positive bacteria, including antibiotic-resistant pathogens such as methicillin-resistant *Staphylococcus aureus*, enterococci, and obligate anaerobes.

The anionic lipopeptide (Fig. 1) consists of a macrocyclic decapeptide core with an exocyclic asparagine linked to a branched-chain fatty acid (C_{14}) containing a Δ*cis3* double bond (48). The peptide core of friulimicin is characterized by the presence of unusual amino acids, such as methylaspartic, D-pipecolinic, and diaminobutyric acids (48) (Fig. 1).

Structurally, friulimicin is related to a number of lipopeptide antibiotics in which individual peptides differ in the exocyclic amino acid and the structure of the fatty acid substituent (3). The characterization of this class of cyclic antibiotics began in the 1950s. Amphomycin was the first lipopeptide to be discovered (17), followed by a number of related antibiotics, including crystallomycin (26), aspartocin (36), glumamycin (14, 37), laspartomycin (30), tsushimycin (38, 39), and the best studied by far, daptomycin (12).

Daptomycin, compared to the true cyclic lipopeptides from the amphomycin and friulimicin group, is classified as a lipodepsipeptide which is further distinguished by the amino acid composition of the peptide core and the existence of three exocyclic amino acids (12).

Daptomycin has been approved for the treatment of skin and skin structure infections as an intravenous formulation in the United States and in Europe and has recently been licensed for the treatment of severe systemic infections caused by resistant gram-positive bacteria, such as staphylococcal endocarditis and bacteremia.

In spite of its success on the market, its mode of action is not fully understood and a molecular target has not been identified so far. Early work demonstrated that the antimicrobial activity of daptomycin strongly depends on the presence of Ca^{2+} (50 μg/ml) (13). According to the multistep model proposed by Silverman et al., daptomycin inserts into the cytoplasmic membrane, with subsequent calcium-dependent integration of the lipopeptide into the membrane followed by oligomerization and disruption of the functional integrity of the cytoplasmic membrane, leading to leakage of potassium ions from the bacterial cell and cell death (41).

More recent functional and structural studies suggest that Ca^{2+} binding of daptomycin occurs in a 1:1 molar ratio in solution, serving to form micelles with an overall positive charge which may deliver high concentrations of daptomycin to the bacterial membrane. In close proximity to the membrane, such micelles may dissociate and daptomycin may insert into the lipid bilayer, resulting in positive membrane curvature and ion leakage (18, 20, 42).

Crystal structure analysis of another lipopeptide, tsushimycin, suggested that in its biologically active form the antibiotic is likely to be a dimer. Dimerization is dependent on the

* Corresponding author. Mailing address: Institute of Pharmaceutical Microbiology, Meckenheimer Allee 168, D-53115 Bonn, Germany. Phone: 49 (0)228 73-5688. Fax: 49 (0)228 73-5267. E-mail: tanja@mibi03.meb.uni-bonn.de.

§ Present address: BRAIN (Biotechnology Research And Information Network) AG, Darmstädter Str. 34, D-64673 Zwingenberg, Germany.

▽ Published ahead of print on 21 January 2009.

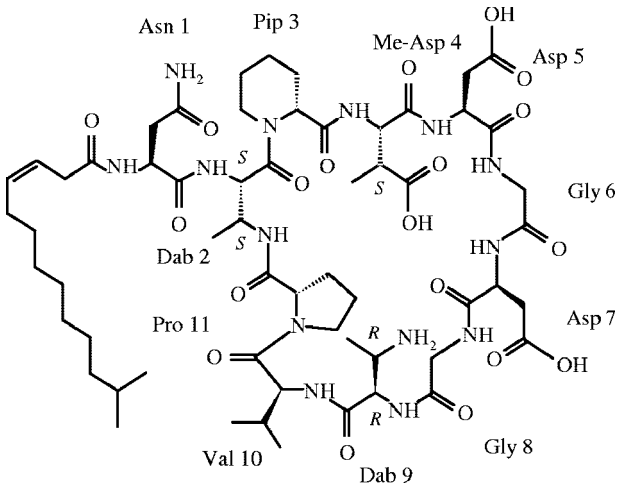

FIG. 1. Chemical structure of the lipopeptide antibiotic friulimicin B. The 10-membered cyclopeptide ring is linked by an exocylic Asn to a branched fatty acid side chain. The positions of the amino acid residues are indicated by numbers next to the amino acid abbreviations. Asn, asparagine; Dab, diaminobutyric acid; Pip, pipecolinic acid; Me-Asp, methylaspartic acid; Asp, aspartic acid; Gly, glycine; Val, valine; Pro, proline.

presence of Ca^{2+}, which results in a structure suitable to accommodate a possible target of either acidic or neutral character (10).

Early studies with amphomycin indicated that the lipopeptide may target bacterial cell wall synthesis, and the possibility has been discussed that it may inhibit phospho-*N*-acetylmuramoyl pentapeptide transferase, which catalyzes the first membrane-associated step in cell wall biosynthesis, linking the soluble UDP-activated cell wall precursor to the membrane carrier. However, molecular details of amphomycin's mode of action have not yet been determined (43, 44, 45).

In this study, we set out to identify the molecular target and the specific mechanism of action of the lipopeptide antibiotic friulimicin B. We found it to form a complex with bactoprenol phosphate without affecting membrane integrity.

Bactoprenol phosphate (C_{55}-P) represents the central lipid carrier of membrane-associated biosynthesis steps in gram-positive bacteria. Besides its function in cell wall biosynthesis, C_{55}-P serves as a lipid carrier for wall teichoic acid biosynthesis and provides polysaccharide transport across the cytoplasmic membrane. Abduction of the C_{55}-P carrier should therefore interrupt precursor cycling and block the synthesis of a functional cell envelope in gram-positive pathogens.

(This study was presented in part at the 47th Interscience Conference on Antimicrobial Agents and Chemotherapy, Chicago, IL, 17 to 20 September 2007 [34]).

MATERIALS AND METHODS

Bacterial strains and growth conditions. *Staphylococcus simulans* 22 was maintained on tryptic soy agar and was grown at 37°C. *Bacillus subtilis* 168 was grown on blood agar at 37°C. Physiological experiments were conducted in cation-adjusted Mueller-Hinton broth (Oxoid, Basingstoke, United Kingdom) unless otherwise stated.

Micrococcus luteus DSM 1790 was used for membrane preparations and was grown at 30°C in tryptone soy broth.

Susceptibility testing. Minimal growth inhibitory concentrations were determined by standard broth microdilution in polypropylene microtiter plates (Nunc brand) using cation-adjusted Mueller-Hinton broth (Oxoid) supplemented with Ca^{2+} (50 μg/ml). Bacteria in the exponential growth phase were diluted to a final inoculum of 10^5 CFU/ml. MICs were read after 16 h of incubation at 37°C.

Antagonization assays. Antagonization of the antibiotics by potential target molecules was performed using standard microdilution methods in polypropylene microtiter plates using cation-adjusted Mueller-Hinton broth (Oxoid) supplemented with Ca^{2+} (50 μg/ml). *S. simulans* 22 was incubated with either 0.625 μg/ml friulimicin B or 0.31 μg/ml daptomycin, corresponding to 8× the MIC. Potential antagonists were added at a fivefold molar excess with respect to the antibiotics, followed by serial twofold dilution. Nisin at 8× the MIC was used as control (2.5 μg/ml).

Precursor incorporation studies. The effect of friulimicin B on the synthesis of macromolecules was studied by monitoring the incorporation of [^{3}H]- or [^{14}C]-labeled precursors (5-[^{3}H]thymidine, [^{3}H]glucosamine hydrochloride, and L-[^{14}C]isoleucine). Overnight cultures of *B. subtilis* 168 and *S. simulans* 22 were grown in CYG (2 g/liter casein hydrolysate, 2 g/liter yeast extract, 5 mM glucose, 10 mM K_2PO_4, pH 7) supplemented with 50 μg/ml Ca^{2+}, and 1 mM of the respective unlabeled metabolite was diluted 50-fold into fresh medium and cultured at 37°C to an optical density at 600 nm (OD_{600}) of 0.5. Cultures were then split into two aliquots, diluted to an OD_{600} of 0.04, and allowed to regrow to an OD_{600} of 0.1. Subsequently, the respective labeled precursor was added to each culture to give a final concentration of 1 μCi/ml; friulimicin was added at 10× the MIC to one aliquot, and the other was run as a control. Incorporation was monitored for up to 2 h. Macromolecules were precipitated with ice-cold trichloroacetic acid (10%) containing 1 mM of unlabeled precursor and incubated for at least 30 min on ice before being filtered through glass microfiber filters (Whatman). The filters were washed with 5 ml trichloroacetic acid (2.5%) containing 50 mM unlabeled metabolite and dried, and incorporation of precursor molecules was counted. Experiments were performed at least three times.

Accumulation of *N*-acetyl-muramoyl pentapeptide. Analysis of the cytoplasmic peptidoglycan nucleotide precursor pool was performed by using *S. simulans* 22 bacteria grown in Mueller-Hinton broth (50 μg/ml Ca^{2+}) to an OD_{600} of 0.5 and supplemented with 130 pg/ml of chloramphenicol. After 15 min of incubation, antibiotics were added at 10× the MIC and incubated for another 30 min. Cells were harvested and extracted with boiling water. The cell extract was then centrifuged, and the supernatant lyophilized. UDP-linked cell wall precursors were analyzed by using high-performance liquid chromatography, and their identities confirmed by mass spectrometry.

Determination of the membrane potential using TPP^+. *B. subtilis* 168 was grown in PYG (2 g/liter peptone, 2 g/liter yeast extract, 5 mM glucose, 10 mM K_2PO_4, pH 7) supplemented with 1.25 mM $CaCl_2$ at 37°C to an OD_{600} of 1, centrifuged, and resuspended at a dilution ratio of 1:3 in fresh medium. To monitor the membrane potential, 1 μCi/ml of [^{3}H]tetraphenylphosphonium bromide (TPP^+; 26 Ci/mMol) was added. The lipophilic TPP^+ diffuses across the bacterial membrane in response to a trans-negative membrane potential. The culture was treated with friulimicin B (10× MIC), and sample aliquots of 100 μl were filtered through cellulose acetate filters (pore size, 0.2 μm; Schleicher & Schüll, Dassel, Germany) and washed twice with 5 ml of 200 mM potassium phosphate buffer. The filters were dried and placed into scintillation fluid, and the radioactivity was measured. The pore-forming lantibiotic nisin (3.6 μM corresponds to 10× the MIC in PYG) or the uncoupler carbonyl cyanide *m*-chlorophenylhydrazone (CCCP; 500 μM) was used as the control.

For calculation of the membrane potential ($\Delta\Psi$), the TPP^+ concentrations were applied in the Nernst equation [$\Delta\Psi = (-2.3 \times R \times T/F) \times \log(TPP^{+\text{inside}}/TPP^{+\text{outside}})$, where T is absolute temperature, R is the universal gas constant, and F is the Faraday constant]. Mean membrane potential values were calculated from the results of four independent experiments.

Potassium release from whole cells. Cells of *S. simulans* 22 were harvested at an OD_{600} of 1.0 to 1.5, washed with cold choline buffer (300 mM choline chloride, 30 mM MES [morpholineethanesulfonic acid], 20 mM Tris, pH 6.5), and resuspended to an OD_{600} of 30. The concentrated cell suspension was kept on ice and used within 30 min. For each measurement, the cells were diluted in choline buffer (25°C) to an OD_{600} of about 3. Peptide-induced potassium leakage was plotted relative to the total amount of potassium release after the addition of 1 μM of the lantibiotic nisin (positive control); the non-pore-forming lantibiotic mersacidin (1 μM) was used as the negative control. Friulimicin B was added at 0.55 μM (10× MIC).

CF efflux from C_{55}-P-containing unilamellar vesicles. Large unilamellar vesicles were prepared by the extrusion technique, essentially as described by Wiedemann et al. (50, 51). Vesicles were made of 1,2-dioleoyl-*sn*-glycero-3-phosphocholine (DOPC) supplemented with 0.1 mol% C_{55}-P (referring to the

TABLE 1. Oligonucleotide primers used in this study

Primer	Sequence[a]
mraY1	5′-ATAGGATCCATTTTTGTATATGCGTTATTAGC GCTAG-3′
mraY2	5′-TCGCTCGAGATGCACTCCAATCCATAAA-3′
murG1	5′-ATAGCTAGCACGAAAATCGCATTTACCG-3′
murG2	5′-CCCCTCGAGATTCAATGCGTCTTTAATCAT-3′
pbp2-1	5′-GCGCTAGCATGACGGAAAACAAAGGATCT-3′
pbp2-2	5′-TTATGTTGAGTCTCGAGGTTGAATATACCTG TTAATCC-3′

[a] Restriction sites used for cloning are underlined.

TABLE 2. MICs (μg/ml) of test strains[a]

Strain	FRI	DAP	NIS
S. simulans 22	0.078	0.039	0.313
B. subtilis 168	0.078	0.625	ND

[a] FRI, friulimicin B; DAP, daptomycin; NIS, nisin.

total amount of phospholipid). Carboxyfluorescein (CF)-loaded vesicles were prepared with 50 mM CF and then diluted in 1.5 ml of K^+ buffer (50 mM MES-KOH, 100 mM K_2SO_4, pH 6.0) at a final concentration of 25 μM phospholipid on a phosphorous base. After peptides were added, the increase in fluorescence intensity was measured at 520 nm (excitation at 492 nm) on an RF-5301 spectrophotometer (Shimadzu) at room temperature. Leakage was documented relative to the total amount of marker release after solubilization of the vesicles by the addition of 10 μl of 20% Triton X-100.

In vitro peptidoglycan synthesis with isolated membranes. In vitro lipid II synthesis was performed using membranes of *Micrococcus luteus* as previously described (9, 33). In short, synthesis was performed in a total volume of 150 μl containing 300 to 400 μg of membrane protein, 10 nmol of undecaprenylphosphate (C_{55}-P), 100 nmol of UDP-*N*-acetylmuramoyl pentapeptide (UDP-MurNAc-pp), 100 nmol of UDP-*N*-acetylglucosamine (UDP-GlcNAc) in 60 mM Tris-HCl, 5 mM $MgCl_2$, pH 7.5, and 0.5% (wt/vol) Triton X-100. UDP-MurNAc-pp was purified as described elsewhere (23). For quantitative analysis, [^{14}C]UDP-GlcNAc (0.5 nmol) was added to the reaction mixture.

Bactoprenol-containing products were extracted with butanol-pyridine acetate (2:1, vol/vol), pH 4.2, and analyzed by using thin-layer chromatography (TLC). Lipid spots were visualized with iodine vapor and excised, and the radioactivity incorporated was counted. Friulimicin and daptomycin were added in molar ratios with respect to the concentration of C_{55}-P.

For purification of milligram quantities of lipid II, the analytical procedure was scaled up by a factor of 500 and purified as described previously (33). Radiolabeled lipid II was synthesized using [^{14}C]UDP-GlcNAc as substrate. Purification of lipid I followed the same protocol except that UDP-GlcNAc was omitted.

Cloning, expression, and purification of cell wall biosynthesis enzymes. The *mraY* gene of *Staphylococcus aureus* NCTC 8325 was amplified with primers mraY1 and mraY2 (Table 1). PCR products and a modified pET20 vector (kindly provided by B. Berger-Bächi, Zürich, Switzerland) were digested by BamHI-XhoI for ligation. In this construct (pTSmraY), the *mraY* gene was expressed under the control of a strong IPTG-inducible promoter, and the encoded MraY protein carried a C-terminal His_6 extension.

The overexpression and purification of the MraY-His_6 fusion protein followed the protocol of Bouhss et al. (7), with some modifications. Briefly, *Escherichia coli* BL21 C43(DE3) (Avidis) cells transformed with the recombinant plasmid pTSmraY were grown in 4 liters 2YT medium (16 g/liter tryptone, 10 g/liter yeast extract, 5 g/liter NaCl, pH 7.5) supplemented with 50 μg/ml ampicillin at 30°C. At an OD_{600} of 0.6 to 0.7, IPTG was added to a concentration of 1 mM, and incubation was continued for 16 h at 25°C to induce expression of the recombinant protein. Cells were harvested (7,000 × *g* for 10 min), washed in 100 ml of 25 mM Tris-HCl, pH 7.5, and resuspended in 10 ml of the same buffer containing 2 mM 2-mercaptoethanol, 150 mM NaCl, 30% glycerol, and 1 mM $MgCl_2$ (buffer A). The cell suspension was sonicated and centrifuged at 100,000 × *g* for 30 min at 4°C in a Beckman type 60Ti centrifuge. The resulting pellet was washed three times with buffer A and subsequently resuspended in 20 ml of the same buffer supplemented with 18 mM *n*-dodecyl-β-D-maltoside (DDM). After incubation for 2 h on ice, the mixture was centrifuged (100,000 × *g* for 30 min at 4°C) to separate membrane debris from solubilized membrane protein. The pellet was subjected to another two solubilization cycles with increasing detergent concentrations (up to 22 mM). The supernatants (S1 to S3) recovered were further purified by using Ni-nitrilotriacetic acid-agarose as described previously (7).

S. aureus NCTC 8325 *murG* and *pbp2* were amplified and cloned into pET21b vector (Novagen) using NheI and XhoI sites (Table 1) to generate C-terminal His_6 fusion proteins. *E. coli* BL21(DE3) (Promega) cells transformed with the appropriate recombinant plasmid were grown in LB medium at 30°C. At an OD_{600} of 0.6, IPTG was added to a concentration of 0.5 mM to induce expression of the recombinant proteins. After 3 h, cells were harvested and resuspended in lysis buffer (50 mM NaH_2PO_4, pH 7.8, 300 mM NaCl, 10 mM imidazole, 1% Triton X-100). Aliquots of 200 mg/ml lysozyme, 100 mg/ml DNase, and 10 mg/ml RNase were added, and cells were incubated for 30 min on ice and sonicated. Cell debris was spun down, and the supernatant was applied to Ni-nitrilotriacetic acid-agarose slurry (Qiagen). This mixture was gently stirred at 4°C for 1 h and then loaded onto a column support. After a washing with lysis buffer, weakly bound material was removed with 50 mM NaH_2PO_4, pH 7.8, 300 mM NaCl, and 20 mM imidazole. His-tagged proteins were eluted with buffer containing 50 mM NaH_2PO_4, pH 7.8, 300 mM NaCl, and 200 mM imidazole. For His-tagged penicillin binding protein 2 (PBP2-His_6), 50 mM Tris-HCl buffer was used as the buffer basis. Purified His-tagged proteins were stored in 50% glycerol at −20°C.

Cloning, expression, and purification of the *S. aureus* peptidyltransferase FemX and the glycyl-tRNA synthetase GlyRS were performed as described previously without any modifications (33).

In vitro peptidoglycan synthesis reactions using purified proteins and substrates. To determine the enzymatic activity of purified MraY-His_6, the assay was carried out in a total volume of 50 μl containing 5 nmol C_{55}-P or [^{3}H]C_{55}-P (14.8 GBq/mmol; Biotrend, Cologne, Germany), 50 nmol of UDP-MurNAc-pp in 100 mM Tris-HCl, 30 mM $MgCl_2$, pH 7.5, and 10 mM *N*-lauroyl sarcosine. The reaction was initiated by the addition of 7.5 μg of the enzyme, and the reaction mixture incubated for 1 h at 37°C.

The MurG activity assay was performed in a final volume of 30 μl containing 2.5 nmol purified lipid I, 25 nmol UDP-GlcNAc or [^{14}C]UDP-GlcNAc in 200 mM Tris-HCl, 5.7 mM $MgCl_2$, pH 7.5, and 0.8% Triton X-100 in the presence of 0.45 μg of purified MurG-His_6 enzyme. The reaction mixture was incubated for 30 min at 30°C.

The assay for synthesis of lipid II-Gly1 catalyzed by FemX was performed as described previously without any modifications (33).

The enzymatic activity of PBP2 was determined by incubating 2.5 nmol lipid II in 100 mM MES, 10 mM $MgCl_2$, pH 5.5, and 0.1% Triton X-100 in a total volume of 50 μl. The reaction was initiated by the addition of 7.5 μg PBP2-His_6, and the reaction mixture incubated for 1.5 h at 30°C.

In all in vitro cell wall synthesis assays, antibiotics were added in molar ratios ranging from 0.5 to 2 with respect to the concentrations of C_{55}-P, lipid I, and lipid II.

Synthesized lipid intermediates were extracted from the reaction mixtures with *n*-butanol-pyridine acetate (1:1, vol/vol), pH 4.2, and analyzed by TLC (see above). Radiolabeled spots were visualized by iodine vapor, excised from the silica plates, and quantified by β scintillation counting (1900 CA Tri-Carb scintillation counter; Packard). Analysis of lipid II polymerization catalyzed by PBP2 was carried out by applying reaction mixtures directly onto TLC plates developed in solvent B (butanol-acetic acid-water-pyridine [15:3:12:10, vol/vol/vol/vol]) and subsequent quantification of residual radiolabeled free lipid II.

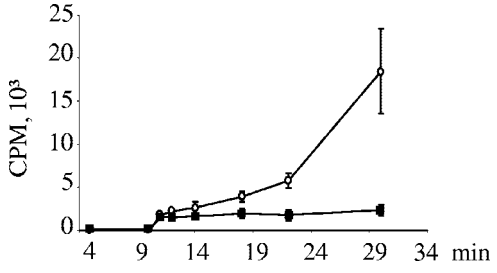

FIG. 2. Impact of friulimicin B on the incorporation of [^{3}H]glucosamine into macromolecules in *B. subtilis* 168. Error bars show standard deviations. ○, untreated controls; ■, friulimicin (10× MIC)-treated cells.

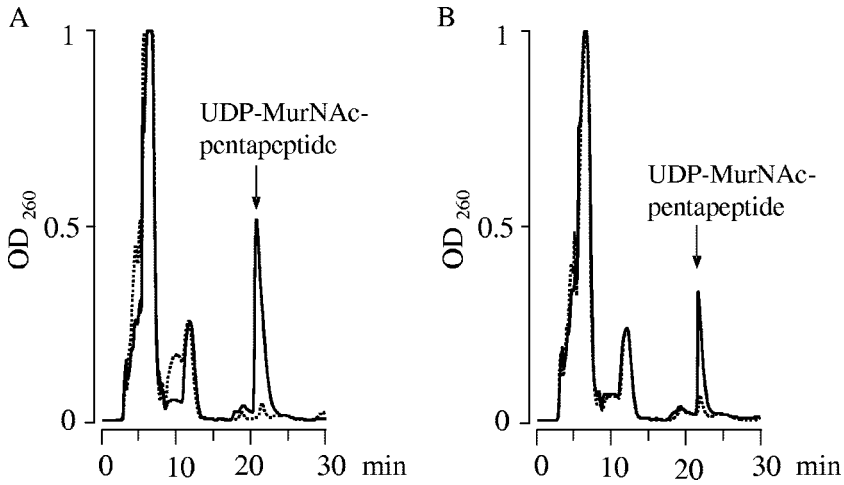

FIG. 3. Intracellular accumulation of the soluble cell wall precursor UDP-MurNAc-pp in S. *simulans* 22. (A) Results for untreated (dashed line) and vancomycin-treated (solid line) cells are shown. (B) Results for friulimicin B-treated (solid line) and daptomycin-treated (dashed line) cells are shown. The experiment was performed with 10× the MIC of each antibiotic for 30 min. Treated cells were extracted with boiling water, and the intracellular nucleotide pool was analyzed by reversed-phase high-performance liquid chromatography. UDP-MurNAc-pp was identified by mass spectrometry.

RESULTS AND DISCUSSION

Effect of friulimicin B on whole cells. Friulimicin B exhibits potent antibacterial activity against a number of gram-positive pathogens, including strains resistant to a wide range of commonly used antibiotics, such as methicillin-resistant *Staphylococcus aureus*, penicillin-resistant pneumococci, and vancomycin-resistant enterococci, as well as difficult-to-treat anaerobic pathogens, such as *C. difficile* (25, 27, 32, 35). In standard microdilution MIC determination assays in polypropylene microtiter plates, friulimicin B inhibited the growth of the test strains used in this study, *S. simulans* 22 and *Bacillus subtilis* 168, at a concentration of 0.078 μg/ml in the presence of calcium (50 μg/ml) (Table 2).

Following macromolecular biosynthesis with radiolabeled precursors, friulimicin at 10× the MIC inhibited the incorporation of glucosamine into cells of *B. subtilis* 168 (Fig. 2), whereas DNA, RNA, and protein biosynthesis were much less affected (data not shown), suggesting cell wall biosynthesis as a potential target pathway.

In order to investigate whether friulimicin interferes with one of the early enzyme reactions of murein biosynthesis, we analyzed the cytoplasmic pool of UDP-linked peptidoglycan precursors in friulimicin-treated cells. Consistent with the results of the *B. subtilis* incorporation studies, friulimicin caused the intracellular accumulation of soluble UDP-linked cell wall precursors, i.e., UDP-MurNAc-pp in *S. simulans* 22, similarly to the vancomycin controls. This finding indicates that UDP-MurNAc-pp, the final soluble cell wall precursor (Fig. 3), is correctly formed in the presence of friulimicin and that one of the subsequent membrane-associated steps of cell wall biosynthesis may be blocked (Fig. 3). In contrast, cells treated with

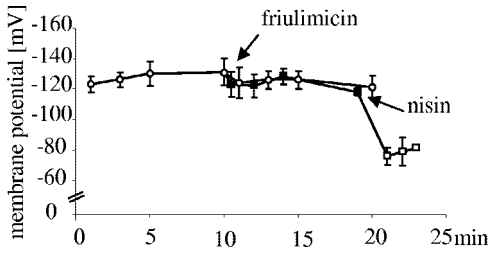

FIG. 4. Impact of friulimicin B on the membrane potential of *B. subtilis* 168. The potential was calculated from the distribution of the lipophilic cation TPP^+ inside and outside the cells. The experiment was started by the addition of TPP^+ to a growing culture; after 10 min of incubation, the culture was divided into two, and one part was run as control (■) while the second was treated with friulimicin (10× MIC) (○). To further control the depolarization assay, the pore-forming lantibiotic nisin (□) was used. Arrows indicate the time points of antibiotic addition. Mean membrane potential values were calculated from the results of four independent experiments. Error bars show standard deviations.

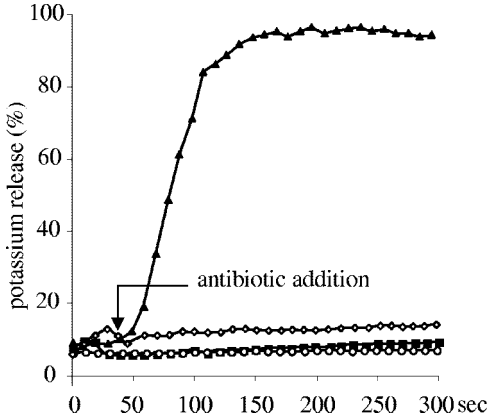

FIG. 5. Impact of friulimicin B on the integrity of the cytoplasmic membrane of *S. simulans* 22 cells. Peptides were added after 30 s, and potassium release was monitored with a potassium-sensitive electrode. Potassium leakage was expressed relative to the total amount of potassium released after the addition of 1 μM of the pore-forming lantibiotic nisin (100%; ▲). The experiment was further controlled with the non-pore-forming lantibiotic mersacidin (1 μM; ◇). ■, untreated cells; ○, friulimicin-treated cells (10× MIC).

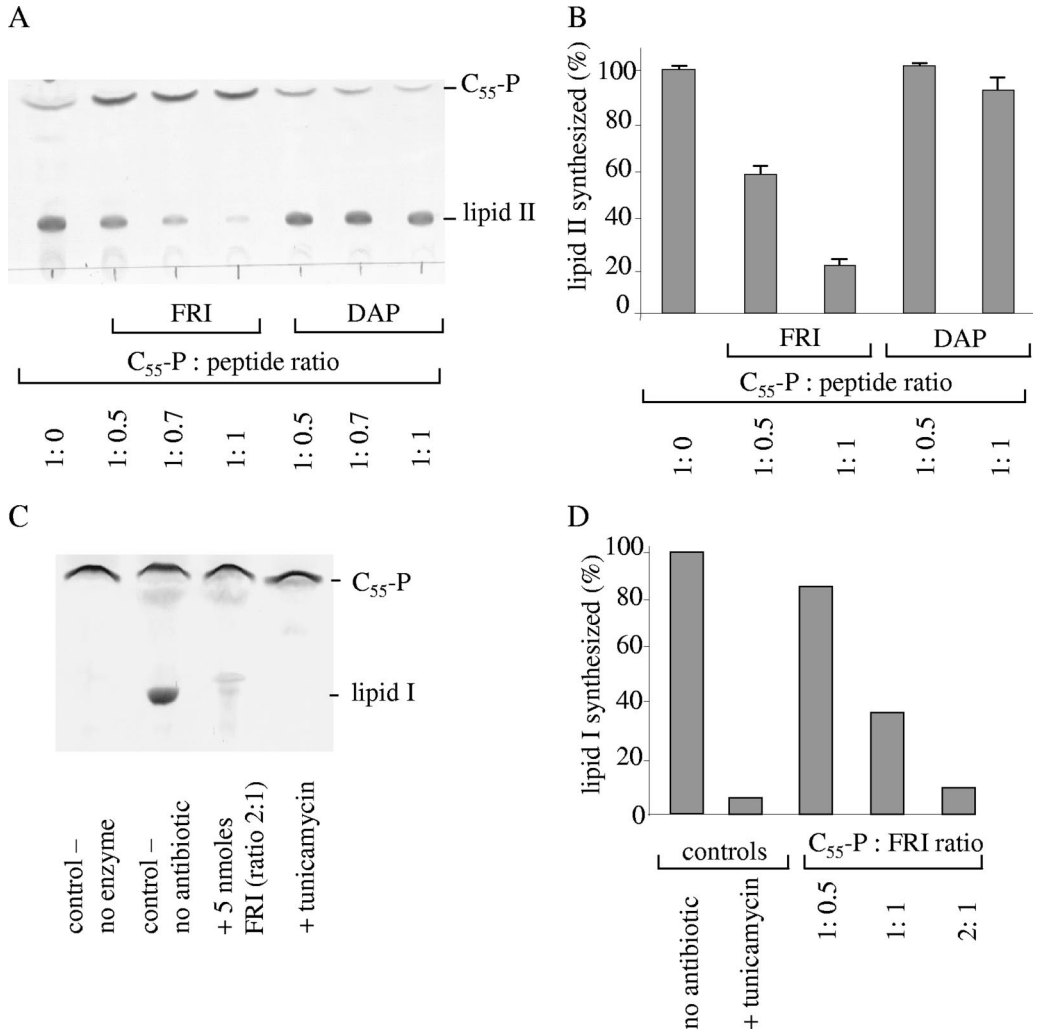

FIG. 6. Impacts of friulimicin B and daptomycin on the membrane-associated steps of cell wall biosynthesis. The peptide was added at increasing molar ratios of 0.5 to 2 with respect to the amount of the substrate C_{55}-P. Reaction products synthesized in the absence of friulimicin were taken as the 100% level. Analysis was performed as described in Materials and Methods. (A, B) Impacts of friulimicin on the overall in vitro lipid II synthesis catalyzed by membrane preparations of *M. luteus*. Reaction products were excised following TLC (A), and the amount of [^{14}C]GlcNAc incorporated was quantified (B). (C, D) Inhibition of the MraY-catalyzed reaction by friulimicin. The conversion of [^{3}H]C_{55}-P to lipid I using purified MraY-His_6 was analyzed in the presence of friulimicin by using TLC (C), and quantification was carried out by analysis of radioactivity incorporated (D). The specific MraY inhibitor tunicamycin was used as a control. Error bars show standard deviations. FRI, friulimicin; DAP, daptomycin; +, present.

daptomycin (10× MIC) in the presence of Ca^{2+} did not accumulate the soluble cell wall precursor (Fig. 3), indicating major differences in the modes of action of the two structurally related lipopeptides.

Unlike daptomycin, which is assumed to form pores (1, 41), friulimicin did not compromise membrane integrity. Membrane pore formation or disruption of membrane integrity should lead to a strong decrease in membrane potential; however, no significant change in membrane potential using TPP^+ was observed after the addition of friulimicin (10× MIC) for a period of 30 min (Fig. 4). Moreover, friulimicin at 10× the MIC did not cause rapid efflux of potassium from intact cells of *S. simulans* 22 (Fig. 5). Even when efflux was monitored over an extended period of 45 min (in the presence of glucose), no significant K^+ release was observed compared to that for the untreated control (data not shown). These data were confirmed by liposome experiments, in which friulimicin was not able to induce efflux of CF (data not shown) even when liposomes were doped with the putative target, C_{55}-P (see below).

Effect of friulimicin B on in vitro cell wall biosynthesis. Based on the information gained from whole-cell assays, we analyzed the impact of friulimicin B on the late, membrane-associated steps of cell wall biosynthesis in vitro. Earlier cytoplasmic steps of cell wall biosynthesis, which had been described to be a potential target site of daptomycin (2, 28), seem unlikely to be targeted by friulimicin since accumulation of UDP-MurNAc-pp was observed after the addition of friulimicin (Fig. 3).

In order to investigate the impact of friulimicin on the late, membrane-associated cell wall biosynthesis steps, we set up in vitro assays to monitor the overall lipid II biosynthesis reaction (Fig. 6A and B) and analyzed the individual steps using purified recombinant enzymes (Fig. 6C and D and 7).

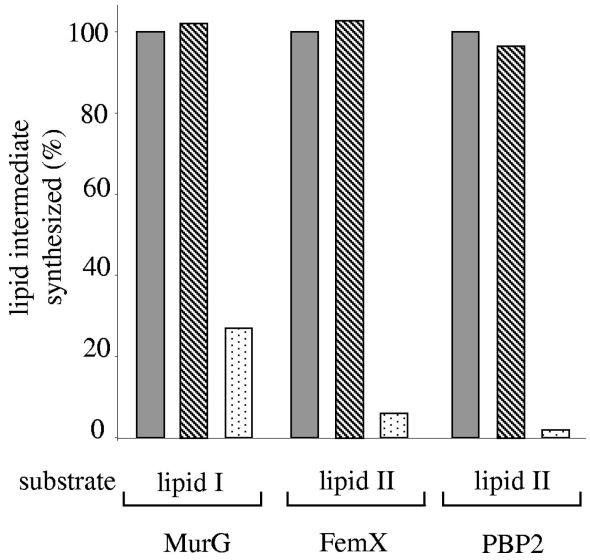

FIG. 7. Effects of friulimicin B on the reactions catalyzed by MurG, FemX, and PBP2. Friulimicin B (striped bars) or nisin (dotted bars) was added to the reaction mixture in a molar ratio of 1:1 or 2:1, respectively, with respect to the concentration of lipid intermediate substrate. Filled bars, untreated control.

The first membrane-associated step of cell wall synthesis is catalyzed by MraY, which transfers the soluble cell wall precursor UDP-MurNAc-pp to the membrane carrier undecaprenylphosphate (C_{55}-P), yielding lipid I (undecaprenylphosphate-MurNAc-pp). The translocase MurG subsequently adds UDP-activated *N*-acetyl-glucosamine (UDP-GlcNAc) to the muramoyl moiety of lipid I, thus yielding lipid II (undecaprenylphosphate-GlcNAc-MurNAc-pp) (47). In staphylococci, the lipid II molecule is further modified by the attachment of a pentaglycine interpeptide bridge, catalyzed by the FemXAB peptidyltransferases (33), before the precursor is translocated across the cytoplasmic membrane where it is then assembled into the growing peptidoglycan network by the action of the PBPs.

Membrane preparations of *Micrococcus luteus* have sufficient MraY and MurG activity for the formation of cell wall precursors lipid I and lipid II in vitro (46). Testing the overall lipid II synthesis reactions with such membranes, to which defined amounts of the soluble precursors UDP-MurNAc-pp and UDP-GlcNAc and the bactoprenol carrier C_{55}-P were added, we found that friulimicin blocked the formation of lipid II. Increasing concentrations of friulimicin led to enhanced inhibition of the lipid II synthesis. Complete inhibition required the addition of at least equimolar concentrations of the lipopeptide and the C_{55}-P carrier (Fig. 6), given the fact that the isolated membranes contain a substantial amount of native C_{55}-P carrier. Similarly to the negative control, in which complete conversion of C_{55}-P to lipid II was achieved, daptomycin had no effect on the overall lipid II synthesis reactions.

In order to get a more detailed insight and to unequivocally identify the step affected, the individual cell wall biosynthesis reaction steps were analyzed using purified recombinant MraY, MurG, FemX, and PBP2 proteins.

In testing the individual reactions, we found the MraY reaction to be inhibited (Fig. 6C and D), whereas the downstream biosynthesis steps catalyzed by MurG, FemX, and PBP2 remained unaffected by friulimicin (Fig. 7).

As demonstrated by TLC (Fig. 6C), recombinant purified MraY-His_6 was able to synthesize lipid I from its substrates C_{55}-P and UDP-MurNAc-pp (lane 2). Complete conversion of the lipid carrier was not attainable because of the reversibility of the reaction (31). Like the specific MraY inhibitor tunicamycin, friulimicin almost completely inhibited the formation of lipid I.

Quantitative analysis of the MraY reaction using radiolabeled C_{55}-P revealed dose-dependent inhibition by friulimicin, and full inhibition was observed at a molar ratio of 2:1 with respect to the concentration of C_{55}-P (Fig. 6D). Friulimicin added in equimolar concentrations inhibited the formation of lipid I to about 60% compared to that in the positive control, where no antibiotic was added. This led us to conclude that friulimicin forms a stoichiometric complex with the bactoprenol carrier in a Ca^{2+}-dependent fashion, rather than interacting with MraY itself. To confirm that the activity of friulimicin does rely on the formation of a complex with bactoprenol phosphate, we performed conventional MIC determinations in the presence of C_{55}-P, C_{55}-PP (undecaprenyl pyrophosphate), lipid I, lipid II, UDP-GlcNAc, and UDP-MurNAc-pp at fivefold molar concentrations with respect to the concentration of friulimicin (Table 3). Only in the presence of C_{55}-P was the activity of friulimicin antagonized, which agrees well with its failure to inhibit the MurG, FemX, and PBP2 reactions, in which lipid I and lipid II are substrates (Fig. 7). Unlike friulimicin, daptomycin had no activity in the overall lipid II biosynthesis assay (Fig. 6A and B) or in any of the specific in vitro assays (data not shown) and was not antagonized by cell wall precursors (Table 3).

Structure and function considerations. For further discussion of the C_{55}-P-friulimicin interaction, it may be instructive to compare the structure of friulimicin with the primary and the published crystal structure of tsushimycin. The two lipopeptides differ only in their extracyclic amino acid, which is aspartate in tsushimycin and asparagine in friulimicin (Fig. 1). The binding stoichiometry of friulimicin to C_{55}-P (2:1) as concluded from the results of the in vitro assay (Fig. 6D) is in accordance with the suggestion that tsushimycin is likely to form a dimer (10). The coordination of the Ca^{2+} ions, a prerequisite for dimerization, is supposed to involve the extracyclic residue, likely via its carbonyl function since the Asp-to-

TABLE 3. Antagonism of antibiotic activity by putative target molecules[a]

Antibiotic[b]	Result[c] with indicated antagonist					
	C_{55}-P	C_{55}-PP	Lipid I	Lipid II	UDP-MurNAc-pp	UDP-GlcNAc
FRI	+	−	−	−	−	−
DAP	−	−	−	−	−	−
NIS	−	−	+	+	−	−

[a] *S. simulans* 22 was incubated with 0.625 μg/ml friulimicin, 0.31 μg/ml daptomycin, and 2.5 μg/ml nisin, corresponding to 8× the MIC; antagonists were added in fivefold molar excess with respect to the concentrations of antibiotics.
[b] FRI, friulimicin B; DAP, daptomycin; NIS, nisin.
[c] +, antibiotic activity antagonized; −, antibiotic activity unaffected.

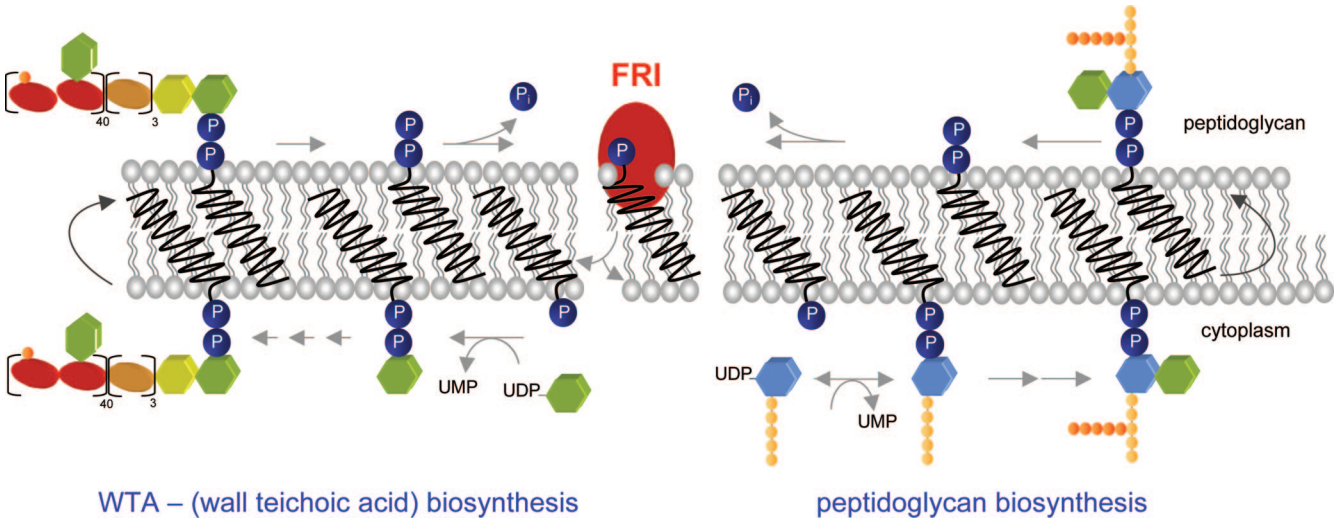

FIG. 8. Model for the mode of action of friulimicin B. We postulate friulimicin B to form a stoichiometric complex with bactoprenol phosphate (C_{55}-P). Abduction of the central carbohydrate carrier interrupts precursor cycling and blocks all biosynthetic pathways which make use of C_{55}-P, such as peptidoglycan (right side), wall teichoic acid (left side), and polysaccharide capsule biosyntheses. The simultaneous interference with these pathways obstructs the formation of a functional cell envelope in gram-positive bacteria. FRI, friulimicin B.

Asn exchange does not seem to make a difference. As pointed out by Bunkóczi et al. (10), the tsushimycin dimer may shape a tunnel-like structure between the monomers, with hydrophobic and hydrophilic areas. Assuming that this model is transferable to friulimicin, such a conformation may be suitable to accommodate the bactoprenol phosphate carrier. Because of the incorporated Ca^{2+}, the openings of the tunnel are positively charged and therefore may participate in the binding of C_{55}-P through interaction with the negatively charged phosphate group. Such a structure may also apply for amphomycin and could explain the observation that this lipopeptide inhibits the formation of dolichyl-P-mannose, dolichyl-P-Glc, and dolichyl-P-P-GIcNAc in eukaryotic membrane systems (4, 21). In light of the recently proposed model for daptomycin (18) that postulates the formation of oligomeric structures, it is interesting to note that the tsushimycin dimers are also likely to assemble into 12-mers which may assume micellar properties (10). These features may also be relevant for friulimicin.

C_{55}-P serves as the central carrier in several processes concerned with membrane trafficking of mono-, di-, and oligosaccharides which constitute the building blocks of bacterial cell walls and capsules. Therefore, it is very likely that friulimicin blocks multiple pathways, as illustrated in the proposed model (Fig. 8). It will be interesting to see whether targeting of C_{55}-P by friulimicin will further lead to a multiplicity of cellular events comprising sequestration of the lipid carrier from the septum area and aberrant cell septation, as observed with some lantibiotics (16).

While our results clearly demonstrate that, in spite of sharing some structural features, friulimicin and daptomycin differ in the molecular mode of antibiotic action, they unfortunately do not provide any hints as to a molecular target for daptomycin in the cell wall biosynthesis pathway, particularly in the membrane-associated steps. Such activities had been suggested in early work on daptomycin (2, 11, 28) and by transcriptional profile analysis of daptomycin-treated *S. aureus* cells (29). In addition, comparative transcriptomic and proteomic analysis of friulimicin versus daptomycin with *B. subtilis* supported such a view (49), although this study also identified differences in the response patterns which point toward distinctions between their antibiotic activities on the molecular level.

Conclusions. This study demonstrates that the lipopeptide antibiotic friulimicin B acts by an unprecedented, cell wall-directed mechanism. Unlike bacitracin, which prevents dephosphorylation of C_{55}-pyrophosphate, friulimicin B specifically forms a complex with the monophosphorylated bactoprenol carrier without affecting membrane integrity. To our knowledge, there is no antibiotic on the market or in clinical development that shares this activity. The clear difference from the molecular mechanisms of daptomycin is also encouraging with regard to the potential development of cross-resistances, since the occurrence of reduced daptomycin susceptibility in *S. aureus* has already been reported (19). Generally, targets such as the sugar-pyrophosphate moiety in lipid II, which is recognized by many lantibiotics (6), and the friulimicin target C_{55}-P described here cannot be altered as easily as protein targets, more-variable sugar moieties, or the D-Ala-D-Ala terminus of lipid II. However, the occurrence of vancomycin-intermediate *S. aureus* strains and strains with reduced susceptibility to daptomycin (19), as well as experimental training of strains toward vancomycin (40) or lantibiotic resistance (24), clearly shows that it is within the physiological capacity of bacteria to adequately respond to such antibiotic stresses and to eventually acquire resistance of sufficient levels for clinical treatment failure. Such adaptation may be more difficult to reach with antibiotics that have complex modes of action based on several killing mechanisms, such as described for the pore-forming and cell wall biosynthesis inhibitory lantibiotics (8, 50). Therefore, it appears an interesting strategy to search for new natural products with such properties, e.g., some glycopeptide antibiotics like telavancin, dalbavancin, and oritavancin (5, 22), or eventually set out to design such multifunctional antibiotics

on a rational basis when more information on molecular mechanisms and targets is available (15).

ACKNOWLEDGMENTS

This work was supported by the BONFOR program of the Medical Faculty, University of Bonn, and by the German Research Foundation (DFG, Sa 292/9-4).

REFERENCES

1. **Alborn, W. E., N. E. Allen, and D. A. Preston.** 1991. Daptomycin disrupts membrane potential in growing *Staphylococcus aureus*. Antimicrob. Agents Chemother. **35:**2282–2287.
2. **Allen, N. E., J. N. Hobbs, and W. E. Alborn.** 1987. Inhibition of peptidoglycan biosynthesis in gram-positive bacteria by LY146032. Antimicrob. Agents Chemother. **31:**1093–1099.
3. **Baltz, R. H., V. Miao, and S. K. Wrigley.** 2005. Natural products to drugs: daptomycin and related lipopeptide antibiotics. Nat. Prod. Rep. **22:**717–741.
4. **Banerjee, D. K.** 1989. Amphomycin inhibits mannosylphosphoryldolichol synthesis by forming a complex with dolichylmonophosphate. J. Biol. Chem. **264:**2024–2028.
5. **Barrett, J. F.** 2005. Recent developments in glycopeptide antibacterials. Curr. Opin. Investig. Drugs **6:**781–790.
6. **Bonelli, R. R., T. Schneider, H. G. Sahl, and I. Wiedemann.** 2006. Insights into in vivo activities of lantibiotics from gallidermin and epidermin mode-of-action studies. Antimicrob. Agents Chemother. **50:**1449–1457.
7. **Bouhss, A., M. Crouvoisier, D. Blanot, and D. Mengin Lecreulx.** 2004. Purification and characterization of the bacterial MraY translocase catalyzing the first membrane step of peptidoglycan biosynthesis. J. Biol. Chem. **279:**29974–29980.
8. **Breukink, E., I. Wiedemann, C. van Kraaij, O. P. Kuipers, H. G. Sahl, and B. de Kruijff.** 1999. Use of the cell wall precursor lipid II by a pore-forming peptide antibiotic. Science **286:**2361–2364.
9. **Brötz, H., M. Josten, I. Wiedemann, U. Schneider, F. Götz, G. Bierbaum, and H. G. Sahl.** 1998. Role of lipid-bound peptidoglycan precursors in the formation of pores by nisin, epidermin and other lantibiotics. Mol. Microbiol. **30:**317–327.
10. **Bunkóczi, G., L. Vertesy, and G. M. Sheldrick.** 2005. Structure of the lipopeptide antibiotic tsushimycin. Acta Crystallogr. D **61:**1160–1164.
11. **Canepari, P., M. Boaretti, M. M. Lleo, and G. Satta.** 1990. Lipoteichoic acid as a new target for activity of antibiotics: mode of action of daptomycin (LY146032). Antimicrob. Agents Chemother. **34:**1220–1226.
12. **Debono, M., B. J. Abbot, R. M. Molloy, D. S. Fukuda, A. H. Hunt, V. M. Daupert, F. T. Counter, J. L. Ott, C. B. Carrell, L. C. Howard, L. D. Boeck, and R. L. Hamill.** 1988. Enzymatic and chemical modifications of lipopeptide antibiotic A21978C: the synthesis and evaluation of daptomycin (LY146032). J. Antibiot. **41:**1093–1105.
13. **Eliopoulos, G. M., C. Thauvin, B. Gerson, and R. C. Moellering, Jr.** 1985. In vitro activity and mechanism of action of A21978C1, a novel cyclic lipopeptide antibiotic. Antimicrob. Agents Chemother. **27:**357–362.
14. **Fujino, M.** 1965. On glumamycin, a new antibiotic. VI. An approach to the amino acid sequence. Bull. Chem. Soc. Jpn. **38:**517–522.
15. **Hancock, R. E., and H. G. Sahl.** 2006. Antimicrobial and host-defense peptides as new anti-infective therapeutic strategies. Nat. Biotechnol. **24:**1551–1557.
16. **Hasper, H. E., N. E. Kramer, J. L. Smith, J. D. Hillman, C. Zachariah, O. P. Kuipers, B. de Kruijff, and E. Breukink.** 2006. An alternative bactericidal mechanism of action for lantibiotic peptides that target lipid II. Science **313:**1636–1637.
17. **Heinemann, B., M. A. Kaplan, R. D. Muir, and I. R. Hooper.** 1953. Amphomycin, a new antibiotic. Antibiot. Chemother. **3:**1239–1242.
18. **Ho, S. W., D. Jung, J. R. Calhoun, J. D. Lear, M. Okon, W. R. Scott, R. E. Hancock, and S. K. Straus.** 2008. Effect of divalent cations on the structure of the antibiotic daptomycin. Eur. Biophys. J. **37:**421–433.
19. **Jones, T., M. R. Yeaman, G. Sakoulas, S. J. Yang, R. A. Proctor, H. G. Sahl, J. Schrenzel, Y. Q. Xiong, and A. S. Bayer.** 2008. Failures in clinical treatment of *Staphylococcus aureus* infection with daptomycin are associated with alterations in surface charge, membrane phospholipid asymmetry, and drug binding. Antimicrob. Agents Chemother. **52:**269–278.
20. **Jung, D., A. Rozek, M. Okon, and R. E. Hancock.** 2004. Structural transitions as determinants of the action of the calcium-dependent antibiotic daptomycin. Chem. Biol. **11:**949–957.
21. **Kang, M. S., J. P. Spencer, and A. D. Elbein.** 1978. Amphomycin inhibition of mannose and GlcNAc incorporation into lipid-linked saccharides. J. Biol. Chem. **253:**8860–8866.
22. **Kim, S. J., L. Cegelski, D. Stueber, M. Singh, E. Dietrich, K. S. Tanaka, T. R. Parr, Jr., A. R. Far, and J. Schaefer.** 2008. Oritavancin exhibits dual mode of action to inhibit cell-wall biosynthesis in *Staphylococcus aureus*. J. Mol. Biol. **377:**281–293.
23. **Kohlrausch, U., and J. V. Höltje.** 1991. Analysis of murein and murein precursors during antibiotic-induced lysis of *Escherichia coli*. J. Bacteriol. **173:**3425–3431.
24. **Kramer, N. E., S. A. van Hijum, J. Knol, J. Kok, and O. P. Kuipers.** 2006. Transcriptome analysis reveals mechanisms by which *Lactococcus lactis* acquires nisin resistance. Antimicrob. Agents Chemother. **50:**1753–1761.
25. **Kresken, M., J. Brauers, B. Körber-Irrgang, H. Labischinski, and S. Pelzer.** 2007. Comparative in vitro activities of the novel antibacterial friulimicin and other antibacterial agents against selected aerobic gram-positive bacteria, abstr. F1-1642. Abstr. 47th Intersci. Conf. Antimicrob. Agents Chemother.
26. **Lomakina, N. N., and M. G. Brazhnikova.** 1959. The composition of crystallomycin. Biokhimiia **24:**425–431.
27. **McGhee, C., T. Bogdanovich, K. Credito, H. Labischinski, and P. C. Appelbaum.** 2007. Activity of friulimicin against glycopeptide and daptomycin non-susceptible *S. aureus*, abstr. F1-1648. Abstr. 47th Intersci. Conf. Antimicrob. Agents Chemother.
28. **Mengin-Lecreulx, D., N. E. Allen, J. N. Hobbs, and J. van Heijenoort.** 1990. Inhibition of peptidoglycan biosynthesis in *Bacillus megaterium* by daptomycin. FEMS Microbiol. Lett. **57:**245–248.
29. **Muthaiyan, A., J. A. Silverman, R. K. Jayaswal, and B. J. Wilkinson.** 2008. Transcriptional profiling reveals that daptomycin induces the *Staphylococcus aureus* cell wall stress stimulon and genes responsive to membrane depolarization. Antimicrob. Agents Chemother. **52:**980–990.
30. **Naganawa, H., M. Hamada, K. Maeda, Y. Okami, T. Takeuchi, and H. Umezawa.** 1968. Laspartomycin, a new antistaphylococcal peptide. J. Antibiot. **21:**55–62.
31. **Pless, D. D., and F. C. Neuhaus.** 1973. Initial membrane reaction in peptidoglycan synthesis. Lipid dependence of phospho-n-acetylmuramyl-pentapeptide translocase (exchange reaction). J. Biol. Chem. **248:**1568–1576.
32. **Schaumann, R., D. Adler, S. Pelzer, H. Labischinski, and A. C. Rodloff.** 2007. Activity of friulimicin and five other antimicrobial agents against 179 gram-positive obligatory anaerobic bacteria, abstr. F1-1644. Abstr. 47th Intersci. Conf. Antimicrob. Agents Chemother.
33. **Schneider, T., M. M. Senn, B. Berger-Bächi, A. Tossi, H. G. Sahl, and I. Wiedemann.** 2004. In vitro assembly of the complete, pentaglycine interpeptide bridge containing cell wall precursor (lipid II-Gly5) of *Staphylococcus aureus*. Mol. Microbiol. **53:**675–685.
34. **Schneider, T., K. Gries, I. Wiedemann, S. Pelzer, H. Labischinski, and H. G. Sahl.** 2007. Friulimicin inhibits cell wall biosynthesis through complex formation with bactoprenol-phosphate, abstr. F1-1640. Abstr. 47th Intersci. Conf. Antimicrob. Agents Chemother.
35. **Schubert, S., A. Dalhoff, S. Pelzer, and H. Labischinski.** 2007. Comparative analysis of the bactericidal activities of friulimicin, daptomycin, tigecycline, and vancomycin against difficult to treat isolates of *S. aureus* and *S. pneumoniae*, abstr. F1-1649. Abstr. 47th Intersci. Conf. Antimicrob. Agents Chemother.
36. **Shay, A. J., J. Adam, J. H. Martin, W. K. Hausmann, P. Shu, and N. Bohonos.** 1960. Aspartocin. I. Production, isolation, and characteristics. Antibiot. Annu. **7:**194–198.
37. **Shibata, M., T. Kanzaki, K. Nakazawa, M. Inoue, H. Hitomi, K. Mizuno, M. Fujino, and A. Miyake.** 1962. On glumamycin, a new antibiotic. J. Antibiot. **15:**1–6.
38. **Shoji, J., and H. Otsuka.** 1969. Studies on tsushimycin. II. The structures of constituent fatty acids. J. Antibiot. **22:**473–479.
39. **Shoji, J., S. Kozuki, S. Okamoto, R. Sakazaki, and H. Otsuka.** 1968. Studies on tsushimycin. Isolation and characterization of an acidic acylpeptide containing a new fatty acid. J. Antibiot. **21:**439–443.
40. **Sieradzki, K., and A. Tomasz.** 1999. Gradual alterations in cell wall structure and metabolism in vancomycin-resistant mutants of *Staphylococcus aureus*. J. Bacteriol. **181:**7566–7570.
41. **Silverman, J. A., N. G. Perlmutter, and H. M. Shapiro.** 2003. Correlation of daptomycin bactericidal activity and membrane depolarization in *Staphylococcus aureus*. Antimicrob. Agents Chemother. **47:**2538–2544.
42. **Straus, S. K., and R. E. Hancock.** 2006. Mode of action of the new antibiotic for Gram-positive pathogens daptomycin: comparison with cationic antimicrobial peptides and lipopeptides. Biochim. Biophys. Acta **1758:**1215–1223.
43. **Tanaka, H., Y. Iwai, R. Ōiwa, S. Shinohara, S. Shimizu, T. Oka, and S. Ōmura.** 1977. Studies on bacterial cell wall inhibitors. II. Inhibition of peptidoglycan synthesis in vivo and in vitro by amphomycin. Biochim. Biophys. Acta **497:**633–640.
44. **Tanaka, H., R. Ōiwa, S. Matsukura, and S. Ōmura.** 1979. Amphomycin inhibits phospho-N-acetylmuramyl-pentapeptide translocase in peptidoglycan synthesis of Bacillus. Biochem. Biophys. Res. Commun. **86:**902–908.
45. **Tanaka, H., R. Ōiwa, S. Matsukura, J. Inokoshi, and S. Ōmura.** 1982. Studies on bacterial cell wall inhibitors. X. Properties of phospho-N-acetylmuramoyl pentapeptidetransferase in peptidoglycan synthesis of *Bacillus megaterium* and its inhibition by amphomycin. J. Antibiot. **35:**1216–1221.
46. **van Heijenoort, Y., M. Derrien, and J. van Heijenoort.** 1978. Polymerization by transglycosylation in the biosynthesis of the peptidoglycan of *Escherichia coli* K 12 and its inhibition by antibiotics. FEBS Lett. **89:**141–144.
47. **van Heijenoort, J., and L. Gutmann.** 2000. Correlation between the structure of the bacterial peptidoglycan monomer unit, the specificity of transpepti-

dation, and susceptibility to beta-lactams. Proc. Natl. Acad. Sci. USA **97:** 5028–5030.

48. **Vértesy, L., E. Ehlers, H. Kogler, M. Kurz, J. Meiwes, G. Seibert, M. Vogel, and P. Hammann.** 2000. Friulimicins: novel lipopeptide antibiotics with peptidoglycan synthesis inhibiting activity from *Actinoplanes friuliensis* sp. nov. J. Antibiot. **53:**816–827.
49. **Wecke, T., D. Zühlke, U. Mäder, S. Jordan, B. Voigt, S. Pelzer, H. Labischinski, G. Homuth, M. Hecker, and T. Mascher.** 2009. Daptomycin versus friulimicin B: in-depth profiling of *Bacillus subtilis* cell envelope stress responses. Antimicrob. Agents Chemother. **53:**1619–1623.
50. **Wiedemann, I., E. Breukink, C. van Kraaij, O. P. Kuipers, G. Bierbaum, B. de Kruijff, and H. G. Sahl.** 2001. Specific binding of nisin to the peptidoglycan precursor lipid II combines pore formation and inhibition of cell wall biosynthesis for potent antibiotic activity. J. Biol. Chem. **276:**1772–1779.
51. **Wiedemann, I., T. Böttiger, R. R. Bonelli, A. Wiese, S. O. Hagge, T. Gutsmann, U. Seydel, L. Deegan, C. Hill, P. Ross, and H. G. Sahl.** 2006. The mode of action of the lantibiotic lacticin 3147: a complex mechanism involving specific interaction of two peptides and the cell wall precursor lipid II. Mol. Microbiol. **61:**285–296.